

## Numerical investigation of polarization-insensitive multiband metamaterial for terahertz solar absorber

I. Hossain<sup>a,\*</sup>, M. Samsuzzaman<sup>b</sup>, M. S. J. Singh<sup>c</sup>, B. B. Bais<sup>c</sup>, M. T. Islam<sup>c</sup>

<sup>a</sup>*Center for Space Science, Institute Perubahan Iklim, Universiti Kebangsaan Malaysia, Malaysia*

<sup>b</sup>*Dept. of Computer and Communication Engineering, Faculty of Computer Science and Engineering, Patuakhali Science and Technology University, Bangladesh*

<sup>c</sup>*Dept. of Electrical, Electronic and Systems Engineering, Faculty of Engineering and Built Environment, Universiti Kebangsaan Malaysia, Malaysia*

This study presents a nanostructured multiband metamaterial absorber for the optical regime application. The proposed structure is exhibited 0° to 90° polarization insensitivity and up to 45° angular stability with more than 90% peak absorption in between 300 THz-800 THz frequency range. Proposed MMA structure is acquired perfect absorption of 99.99% at 571 THz, 99.50% at 488.26 THz, 99.32% at 598 THz frequency by adjusting geometrical parameters. Due to perfect impedance matching with plasmonic resonance characteristics, these structures achieved an average absorption of 95.30%, 91.96%, 97.25%, 97.65%, 91%, 90%, 90.23% in between (337.5 THz-346.5 THz), (471 THz-478 THz), (497.5 THz-505 THz), (519 THz-530.5 THz), (564.5 THz-577 THz), (604 THz-673 THz), (686 THz-708 THz), respectively. The near field pattern of proposed MMA is used to explain the absorption mechanism at resonance frequency point and the geometric parameters are explored and analyzed to demonstrate the performance of the proposed structure. Moreover, CST-HFSS interference is validated the simulation data with the help of the finite element method (FEM). Polarization insensitivity and wide angular stability in terahertz (THz) frequency regime make this structure suitable for the application of magnetic resonance imaging (MRI), color images, thermal imaging and solar cell applications like exploitation of solar energy.

(Received December 18, 2020; Accepted May 5, 2021)

*Keywords:* Polarization-Insensitive, Multiband Metamaterial, Terahertz, Solar Absorber

### 1. Introduction

Metamaterials have entered the modern particularly dominant electromagnetism, high-frequency engineering, and materials science research inside a comparatively short period. Exceptionally much too prior thinks about, it has overseen to discover a particular profile and visibility inside the primary decade of 21<sup>st</sup> century. In recent years, metamaterials have attained incredible consideration by researchers because of their exceptional electromagnetic properties spreading over the entire optical ranges extend that caused different types of technological application [1-3].

For a substantial variation in metamaterials operating frequency, wavelength free space should remain high in the unit cells [4]. This particular characteristic enables metamaterials to be used as antennas [5], waveguides [6], invisibility cloaking [7], absorption [8], various kinds of sensors [9], planer filers [10], super lensing [11], medical imaging [12]. The visible and infrared ranges are covered by narrow bandwidth metamaterial absorber (MMA) to the perspective of

---

\* Corresponding authors: ismailiuc555@gmail.com

absorption bandwidth [13]. First metamaterial absorbers at the terahertz frequency region were made and demonstrated by [14]. Broadband absorbers in metamaterials are the main causes of incident radiation material properties that are independent of frequency [15]. Periodic structure based metamaterial shows a high absorbance [16]. For this reason, as opposed to small thicknesses materials, this material high frequency could take the form of terahertz to the infrared through a simpler design and less expensive manufacturing process [17]. At the visible wavelength from 400 nm to 700 nm almost 80% average absorption has been found with the Cu/Si<sub>3</sub>N<sub>4</sub>/Cu stack coating on a silicon substrate [18]. Damper dual-band four-layer gold, gallium arsenide (GaAs), and Pyrex (glass) demonstrated 99.99% and 99.90% absorbance [19]. Harvesting energy from indoor and outdoor source in between 300-3000 nm wavelength photovoltaic plays significant rules [20]. The two dimensional (2D) materials have been significantly alternation for several photonic based applications due to their exclusive optical and electrical properties [21, 22].

A compact, ultrathin metamaterial broadband absorber MMBA has proposed this study to harvesting solar energy at the visible and infrared spectrum. The proposed structure shows an average absorption above 90% in between 300 THz-800 THz frequency spectrums. Proposed designed structure is exhibited 0° to 90° polarization-sensitivity and more than 45° angular stability both in TE and TM mode of propagation at the terahertz (THz) frequency ranges. The most effective absorption mechanisms, BPA change the shape by simply regulating the unit cells' parameters and relatively optimized the dielectric layer. A metal ground plane can reduce reflection and transmission to maximize absorption.

## 2. Structure design and model

The geometrical layout of the proposed MMA unit cell is explained in this section, this structure has three layers (metal-dielectric-metal) and a dielectric layer is sandwiched between a metal layer and resonator layer. The dielectric layer is made of quartz (fused) having loss tangent and electric permittivity 0.0001, 2.4. The dielectric (quartz) layer is a continuous board which can block the transmission of the incident light, and this layer is a pattern layer. Proposed MMA has an equal dimension of length and width denotes by “a=1000 nm”. The top metasurface is comprised of a tungsten-based bow-shape circulator resonator and the bottom layer is also made of tungsten. The entire four bows like shape have an equal dimension of “d=649.31”, after that plus shape is designed at the center than four arrow shape is designed around the plus shape. The dimensions of plus shape are denoted by b and c, these parameters values are 60 nm, 100 nm”, respectively. Around the plus (+) shape four arrows like shape are designed as the name of the left arrow, right arrow, up arrow and down arrow and all the arrow shape has an equal dimension of “e=96.60”. Fig. 1(a-c) respectively corresponds to the front view, side view and isometric view of the MMA unit cell. The thickness of the resonator is defined as  $t_r=15$  nm, dielectric layer  $t_d=60$  nm and metallic layer  $t_m=150$  nm, respectively. This structure is used metallic to obtain zero transmission, the tungsten continuous layer of Fig. 1(b). The thickness of the back-layer metal plate is maintained a level greater than the proposed MMA unit cell skin depth ( $\delta$ ) to ensure the zero transmission in the optical region is defined as, Skin depth,  $(\delta) = \sqrt{2\rho / 2\pi f \mu_R \mu_0}$  Herein, conductivity and permeability of back-layer metal plate denoted by  $\rho$  and  $\mu_R$  as well as permeability in free space denoted by  $\mu_0$ . However, Total thickness of the proposed structure is 225 nm also it's considered as ultra-thin which can be easily rolled on the thermo photovoltaic solar cell (STPV).

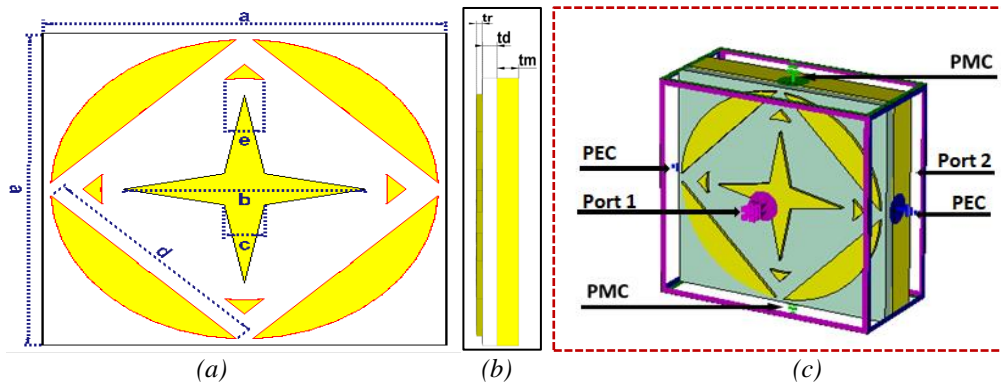
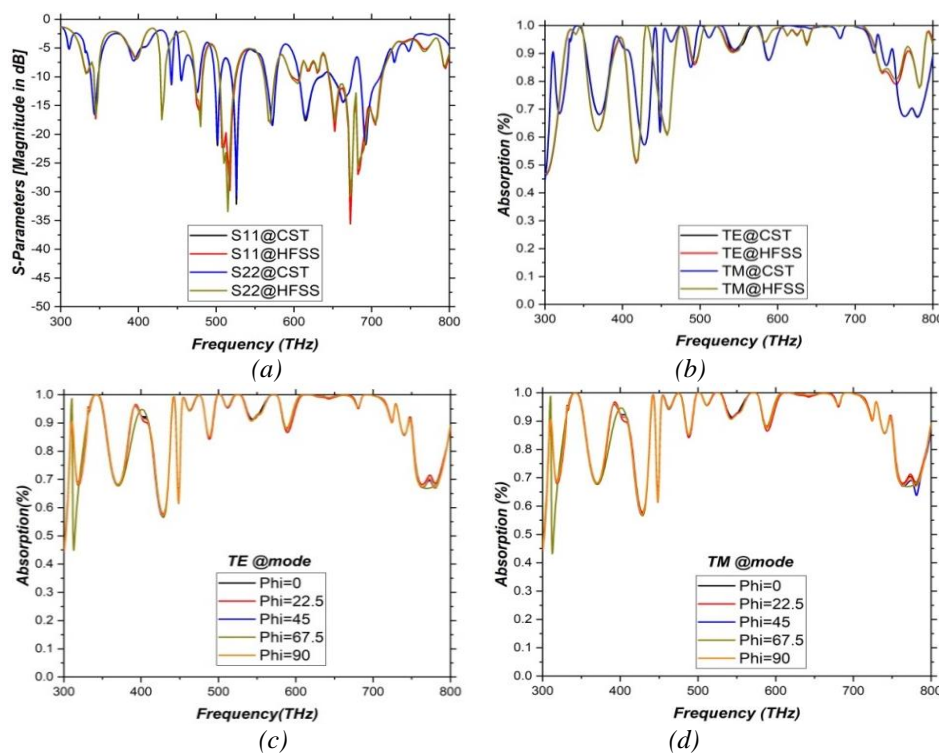


Fig. 1. Schematic diagram of the proposed structure (a) Front view (b) Side view (c) Isometric vies.

Proposed design simplest highlights the transverse electric (TE) and transverse magnetic (TM) mode. The direction of x-axis and y-axis are considered for transverse electric (TE) and transverse magnetic (TM) mode of propagation and the z-axis are taken into consideration as an open area in which frequencies will bypass over the structure. The structure is simulated by a study of microwave technology numerical computer simulation (CST) tools. Data analysis is conducted and a graph is produced with interference CST-Origin validated in results and discussion section.

### 3. Results and discussion

Simulated absorption curve of the proposed structure is presented in Fig. 2(b). Perfect absorption in metamaterial can be calculated by the equation, Absorption,  $A(\omega) = 1 - S_{11}^2(\omega) - S_{21}^2(\omega)$  where  $S_{11}$  is scatters parameters for reflection coefficient and  $S_{21}$  for transmission coefficient. The scatters parameters are exhibited in Fig. 2(a) magnitude in dB scale.



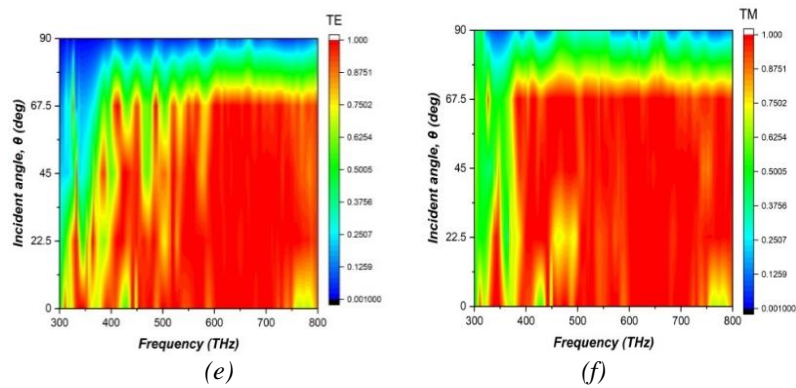


Fig. 2. (a) Comparison of  $S$  parameter of TE and TM mode in CST and HFSS (b) Comparison of absorption in between CST Vs HFSS at (c) TE and (d) TM mode, (e) Polarization sensitivity at TE mode, (f) TM mode.

The realization of the zero reflection can be achieved if the impedance is matched perfectly in the air. The metamaterial structure designed indicates the ability to raise nearly 100% absorption in different discrete frequency points at 501 THz, 526 THz, 572 THz, and 692 THz. This selected frequency point localized resonances of the proposed structures and thus the proposed structure allows controlling and adjusting resonance frequency of indicated point shows in Figure 2 (b), which can play an important role in practical applications. In Figure 2(c) and (d) is demonstrated the polarization insensitivity both of TE and TM mode of propagation. Furthermore, the proposed MMA unit cell response up to  $45^\circ$  angular stability shows in Figure 2(e) and (f), respectively for TE and TM mode. Sweep parameters are very helpful for determining the best absorption of the design and utilization; here some significant parameters are sweep to find out the perfect absorption. Significant parameter is sweep associated with the thickness of dielectric layer "td"; modifying this value from 100-150 nm, observed a most important adjustment in the absorption mechanism. Various thicknesses (100, 120, 150) of the dielectric layer has appeared with absorption values of 95.84%, 92.20%, 98.75%, and 99.99% at the frequency point of 400 THz, 770 THz, 600 THz, and 550 THz.

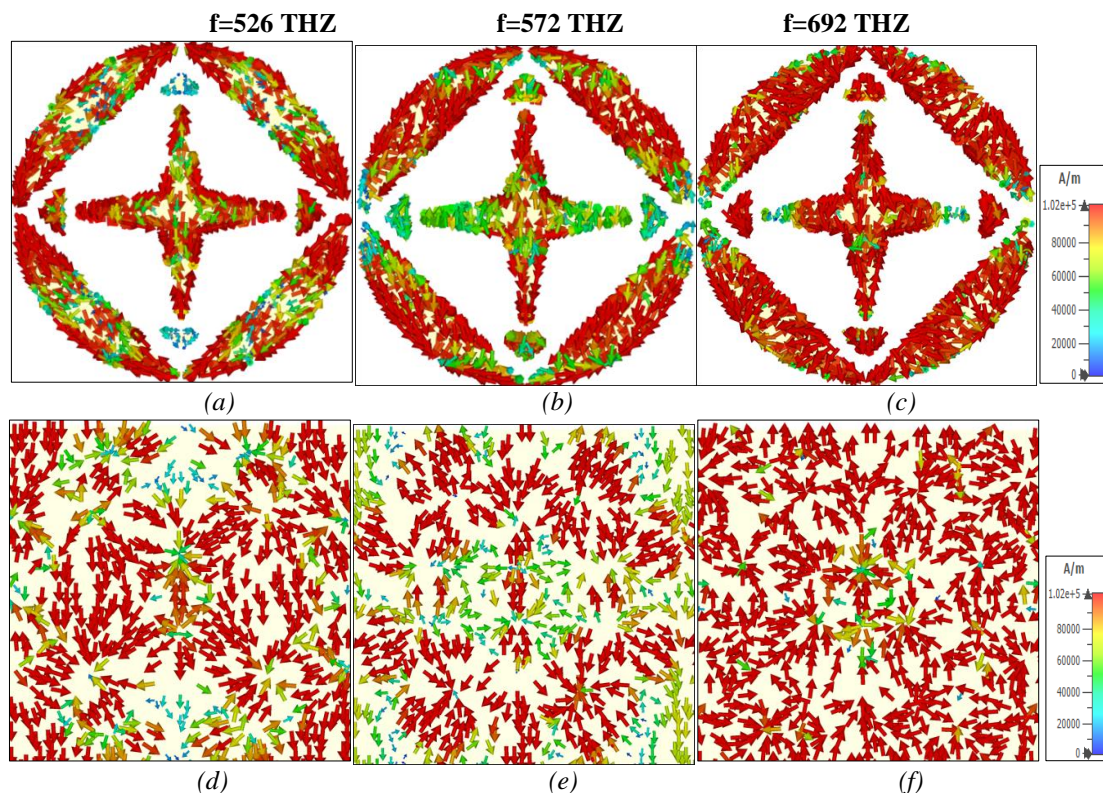


Fig. 3. (a) Front layer surface current density at 526 THz (b) 572 THz, (c) 692 THz, (d) Back layer surface current density at 526 THz, (e) 572 THz and (f) 692 THz.

The capacitance substance between metallic and resonator is an alternative by the width of certain dielectric layers. Diminish within the capacitance the resonance frequency is expended. This singularity may be utilized inside optical sensors or identify the thickness of any kind of dielectric layer. Specific dielectric layer thicknesses variations can be clarified by changes in the resonator capacitance with adjusting variables. The selection of metasurface thickness " $tr=15$ " has a significant to achieve the perfect absorption with fairly large bandwidth. Moreover, the resonator and metallic made of capacitance and inductance are relatively in thickness. Surface current, electric (E) field and magnetic (H) field are analyzed in this section to comprehend the mechanism of absorption. In Figure 3 (a)-(f) is exhibited the surface current of resonator and back-layer at three peak absorption frequencies (526 THz, 572 THz, 692 THz). Moreover, at this three different frequencies E field and H field are also analyzed shows in Figure 4 (a)-(f). Tow current loop (clockwise and anticlockwise) is observed every bow-like shape at 526 THz frequency shows in Figure 3 (a) but at this frequency in plus like shape located at the center of the proposed unit cell is exhibited antiparallel current flow direction. From the center of the bow-like shape, the clockwise and anticlockwise current direction is considered, the right-hand current loop is considered as clockwise whereas the left-hand current loop is considered as the anticlockwise current loop. The low intensity of current has less significant over the magnetic (H) field, the anticlockwise current has a low intensity that why it has less significant. Edge of the four bows like shape shows the high intensity of current and its effect the magnetic field. Close observation of the metal layer current shows that this current is anti-parallel compared to the next flow so that the magnetic dipole resonance can be formed.

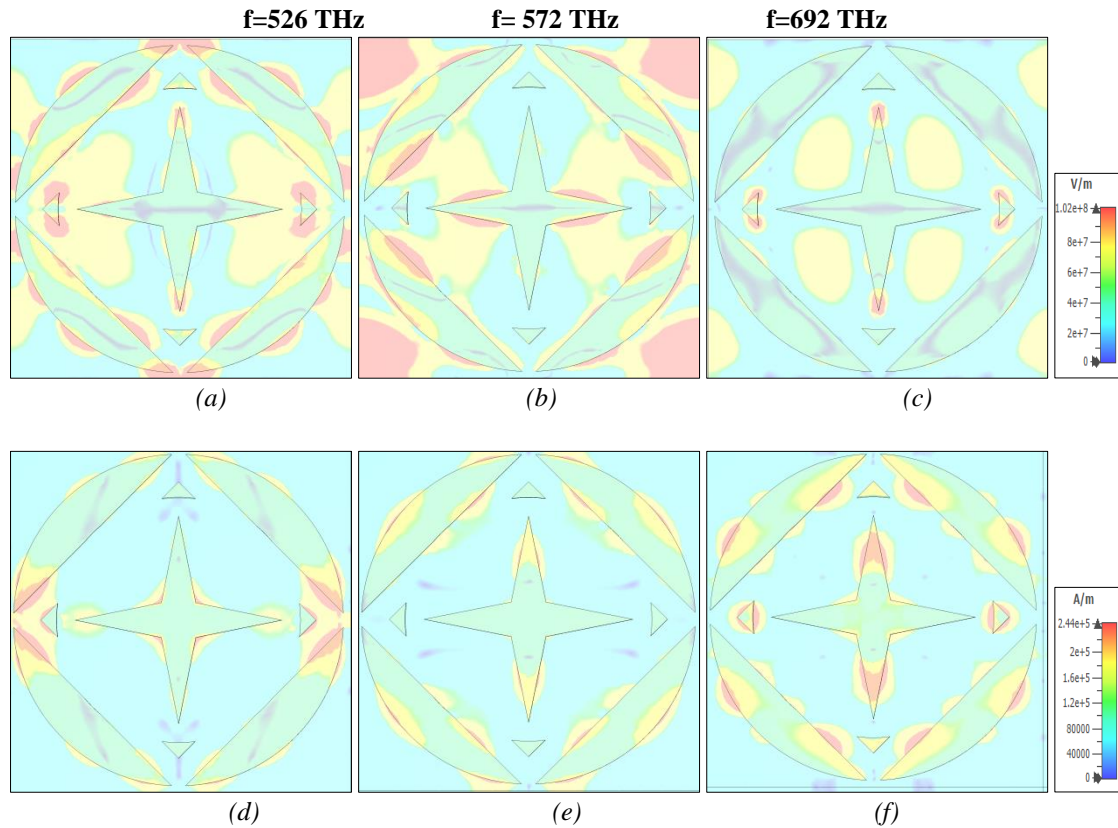


Fig. 4. (a) E-field at 526 THz (b) E-field at 572 THz, (c) E-field at 692 THz, (d) H-field at 526 THz, (e) H-field at 572 THz and (f) H-field at 692 THz.

Back metal layer current show antiparallel compared with resonator layer thus formed magnetic dipole resonance. At 572 THz frequency show more directional current but it is observed that the random nature of surface current is minimized and concentrate high current is noticed at 692 THz. At the point of up arrow-like shape and down arrow-like shape shows currents density is low. Figure 3 (f) represent surface current density at 692 THz in the back metal layer. Figure 03 (f) exposes, the back metal plane current is antiparallel at the localized front currents thus magnetic resonance occurs and this localized magnetic field is the reason for the high magnetic field at this frequency. Electric field (E) of these frequencies points are trapped in the edges of the tungsten resonator and three resonance frequency point shown in Figure 04 (a)-(c). To raise the absorption performance of the proposed structure, origin of the resonance frequency point should be originated from the localized structure but the field trapped positions are different. Magnetic field (H) patterns of the light absorber at the resonance frequency point are illustrated in Figure 04 (d)-(f). Based on the above analysis, it can easily understand why the parameter variations of the three resonators affect the performance of multiband light absorber. Thus this front and back antiparallel current again produce two strong magnetic (H) fields at the two horizontal curving points as shown in Figure 4(d). This back current cooperates with the front current to create magnetic resonance again, the places where front and back currents are antiparallel strong magnetic field is observed at those portions of the unit cell as shown in Figure 04 (f). This strong magnetic field interacts with the incident electromagnetic waves and thus helps to obtain a high level of absorption in this frequency. Proposed structure is achieved a remarkable absorption within the frequency spectrum 300 THz-800 THz. The evaluation of the proposed design and the previous work is demonstrated in Table 01.

Table 1. Comparison of previous work which is included in reference section.

Reference No.	Operating range (THz)	Absorption efficiency	Angular stability
1	293.9-624.5	80%	-
2	220-360	90%	35°
8	548-669	90%	-
17	54.5-29.9	99%	50°
This work	300-800	99%	45°

#### 4. Conclusions

The use of the metasurface configuration based on the tungsten of the absorber would give broadband spectral absorption characteristics in the optical regime. The results exhibited up to 99% absorption in the frequency spectrum of 400 to 750 THz. The obliqueness of the incidence affects the magnitude of the absorption that preserves the broadband characteristic. However, cases of normal events show maximum absorption; increased angle of events from 10 ° to 60 ° decreased absorption of ~ 20%.

The proposed MMA is exhibited up to 45 ° angular stability with 0 ° to 90 ° polarization insensitivity. The interference of computer simulation software (CST) and high-frequency simulation software (HFSS) is validated these simulated data. The graphical data is arranged by using Origin Pro software. A numerical investigation is validated this multiband light absorber. The study also combines optimization of geometric parameters and FMA operating conditions by determining the figure of merit (FOM) and operational bandwidth (OBW).

#### Acknowledgement

This work is supported by the Universiti Kebangsaan Malaysia (UKM), Malaysia Research Grant code GUP-2020-008.

#### References

- [1] N. Mou, X. Liu, T. Wei, H. Dong, Q. He, L. Zhou et al., *Nanoscale* **12**, 5374 (2020).
- [2] A. Alam, S. S. Islam, M. Islam, A. F. Almutairi, M. T. Islam, *Materials* **13**, 2560 (2020).
- [3] S. Mahmud, S. S. Islam, A. F. Almutairi, M. T. Islam, *IEEE Access* **8**, 129525 (2020).
- [4] D. Smith, D. Vier, T. Koschny, C. Soukoulis, *Physical review E* **71**, 036617 (2005).
- [5] M. M. Hasan, M. R. I. Faruque, M. T. Islam, *Scientific reports* **8**, 1 (2018).
- [6] F. Fan, X. Zhang, S. Li, D. Deng, N. Wang, H. Zhang et al., *Optics express* **23**, 27204 (2015).
- [7] S. S. Islam, M. R. I. Faruque, M. T. Islam, *Materials* **8**, 4790 (2015).
- [8] M. Bağmancı, M. Karaaslan, E. Ünal, O. Akgöl, C. Sabah, *Optical and Quantum Electronics*, **49**, 257 (2017).
- [9] G. Duan, J. Schalch, X. Zhao, J. Zhang, R. Averitt, X. Zhang, *Actuators and Microsystems (Transducers)*, 1999 (2017).
- [10] M. Ghasemi, M. Baqir, P. Choudhury, *IEEE Photonics Technology Letters* **28**, 1100 (2016).
- [11] F. Li, J. Deng, J. Zhou, Z. Chu, Y. Yu, X. Dai et al., *Scientific reports* **10**, 1 (2020).
- [12] Z. Liu, M. Shimizu, H. Yugami, *Optics Express* **28**, 5812 (2020).
- [13] S. Korkmaz, M. Turkmen, S. Aksu, *Sensors and Actuators A: Physical* **301**, 111757 (2020).
- [14] H. Tao, N. I. Landy, C. M. Bingham, X. Zhang, R. D. Averitt, W. J. Padilla, *Optics express* **16**, 7181 (2008).
- [15] C. M. Watts, X. Liu, W. J. Padilla, *Advanced Materials* **24**, OP181 (2012).

- [16] A Hoque, M.T. Islam, A.F. Almutairi, M.E.H. Chowdhury, M. Samsuzzaman, Scientific Reports **10**, 1 (2020).
- [17] Y. Zhang, T. Li, Q. Chen, H. Zhang, J. F. O'Hara, E. Abele et al., Scientific reports **5**, 18463 (2015).
- [18] P. Zhu, L. Jay Guo, Applied Physics Letters **101**, 241116 (2012).
- [19] P. Rufangura, C. Sabah, Vacuum **120**, 68 (2015).
- [20] F. Mateen, M. A. Saeed, J. W. Shim, S.-K. Hong, Solar Energy **207**, 379 (2020).
- [21] Z. Xie, Y.-P. Peng, L. Yu, C. Xing, M. Qiu, J. Hu et al., Solar RRL **4**, 1900400 (2020).
- [22] Z. Xie, Y. Duo, Z. Lin, T. Fan, C. Xing, L. Yu et al., Advanced Science **7**, 1902236 (2020).